



Nonlinear Dynamics of Electron Pitch Angle Scattering in the Earth's Magnetosphere: A Study of Whistler-Mode Wave Interaction under Varying Plasma Conditions

Chelimella Kishan ^{1*}, Dr. Arvind Kumar ²

1. Research Scholar, Shri Krishna University, Chhatarpur, M.P, India

chelimella.kishan@gmail.com ,

2. Associate Professor, Shri Krishna University, Chhatarpur, M.P., India

Abstract: As a result of resonant interactions with the magnetosphere, electron pitch angle scattering the whistler-mode waves is important for the dynamics of energetic electrons and for the space weather effects. The complex behavior of such interactions as a function of plasma state, using analytical theories and computer simulations. The analysis of the results shows that plasma density, wave amplitude, and the changes in the geomagnetic field play a crucial role in the rates of electron scattering and precipitation. Thus, the main focus of the research is made on the transition between linear and nonlinear regimes with reference to the loss of energetic electrons. This work helps to advance the knowledge of magnetospheric dynamics and has implications for satellite protection, radiation belt evolution, and space weather prediction. The results fill the gaps in existing models and serve as a basis for subsequent research in plasma physics and magnetospheric science.

Keywords: Electron Pitch Angle Scattering, Whistler-Mode Waves, Magnetosphere, Nonlinear Dynamics, Plasma Conditions

----- X -----

INTRODUCTION

Magnetosphere of the Earth is a complex and active area, where electrons and ions and electromagnetic waves react with each other. Of these, whistler-mode waves, which are particularly crucial in defining the actions of the powerful electrons are very low-frequency electromagnetic waves (Behar, 2020). These waves which are natural and man-made disturb the path of electrons from the magnetic field through something known as pitch angle scattering (Blum et al., 2021). This phenomenon is quite essential for the knowledge of the radiation belt's dynamics, space weather events, and practical functioning of satellites. The whistler-mode wave–electron interaction is described by nonlinear dynamics, which go beyond the linear analysis (Borovsky & Valdivia, 2018). These interactions exhibit a strong dependence on plasma parameters, such as density, temperature and magnetic field. Fluctuations of these parameters affect the scattering rates and the subsequent the release of charged particles into Earth's atmosphere affecting ionospheric chemistry and communication systems (Bortnik, 2022). The nonlinear behavior of electron pitch angle diffusion in the magnetosphere as a function of plasma density. Using state of the art simulation tools and analysis it investigates how plasma density, wave intensity and magnetic fields alter the efficiency and nature of scattering (Bortnik, Inan, & Bell, 2002). The results are expected to contribute to a better understanding of the complex dynamics of wave-particle interactions and their consequences for space

weather forecasting and management (Bortnik, Thorne, & Inan, 2008).

LITERATURE REVIEW

Smith et al. (2021) studied the nonlinear dynamics of electron pitch angle scattering in the magnetosphere. In their study, they emphasized on the role of whistler-mode waves in controlling electron motion especially in relation to plasma density fluctuations. Through the particle-in-cell simulations, they showed that nonlinear effects cause increased scattering efficiency, especially at low latitudes. This work highlighted the importance of considering non-linearities when making space weather models and their effects on satellites.

Chen and Zhao (2020) investigated the characteristics of whistler-mode waves in relation to the scattering of energetic electrons at different pitch angles. Researchers used data collected by the Van Allen Probes to examine wave-particle interactions in various geomagnetic settings. Electron scattering rates are strongly affected by wave strength and frequency spectrum, according to their research. The mechanisms controlling electron precipitation and its effects on radiation belt structure were illuminated by this study.

Li et al. (2019) investigated how oblique whistler-mode waves affected the dispersion of pitch angle in the inner radiation belt. Additionally, they statistically proved that, particularly for high-energy electrons, oblique waves had better diffusion than parallel waves. As the primary determinant of the spatial density of trapped electrons and an improvement in radiation belt predictions, their research centered on the wave normal angle.

Anderson and Baker (2018) studied the impact of variations in plasma density on the interaction between waves and particles in the magnetosphere. Additional findings include the fact that density gradients have a significant impact on whistler-mode waves' propagation characteristics and electron scattering capabilities. They used theoretical modeling and analysis of satellite data to conclude that in order to study electron behavior during geomagnetic storms, one needs accurate measurements of plasma density.

Zhang et al. (2015) offered an extensive review of nonlinear wave-particle interactions in the magnetosphere using wave amplitude and frequency modulation. In their work, they showed that nonlinear effects can cause resonance broadening that in turn increases the pitch angle scattering over a wider range of energy. This research provided the foundation for studying the detailed interactions of waves and particles and how they can be used for radiation belt analysis.

RESEARCH METHODOLOGY

Experiments conducted with the OGO-6 satellite have shown substantial ELF hiss emissions at 450 km in the inner radiation belt when the geomagnetic field is in a state of flux. A band-width of 300 Hz and an average peak power spectral density of $4 \times 10^{-7} \text{ T}^2 \text{ Hz}^{-1}$ were characteristics of the emissions that were detected. We are assuming a 5 dB augmentation and projecting this intensity onto the equatorial plane since our analysis will include pitch angle scattering and diffusion at $L = 1.2$ in the equatorial area. When L

$= 1.2$, the extrapolated intensity is determined to be $1.26 \times 10^{-6} \gamma^2 \text{ Hz}^{-1}$ at 550 Hz, with an estimated wave field of 19.44 MHz. The ARIEL 3 satellite measured the magnetic field strength at 500 km in the

ionosphere, and from those measurements, the wave field at the whistler frequency of 3.2 kHz was determined. An estimated 5.25 x 100 Hz wave is propagating in the ionosphere at 500 km (L = 1.2). If this is projected onto the equatorial plane and amplified by 10 dB, its intensity will increase to 5.25 x 10² Hz. When operating at 1 kHz, this produces a wave field of 2.29 m. A newly observed powerful 5 KHz VLF hiss with a peak strength of 10 W m² Hz and a bandwidth of 2 kHz was picked up by the Kagoshima ground station (L = 1.2) in Japan. There is a 15 dB rise when the observed intensity on the ground is extrapolated to the equatorial plane. The resulting wave field is, and the measured equatorial intensity at L 1.2 is m²² Hz (2.14 x 10¹⁰ 2 3.16 x 10¹⁵ W m 0.66 m y. Hz). We have taken into account an extrapolation of intensity of 5, 10, and 15 dB at 550 Hz, 3.2 kHz, and 5 KHz, respectively, when we reach the equatorial plane. The reason for this is because, according to Somayajulu and Tantry (1967), propagation loss becomes worse as the wave frequency gets higher. Specifically, in the lower ionosphere zone, waves with a frequency of 5 kHz encounter an extra 5 dB of propagation loss.

Based on the energy flux profiles from in situ observations aboard the HITCHHIKER1 (196325 B) spacecraft in the inner radiation zone, we assume an energetic electron flux of 1 x 10 el. cms sterad (L = 1.2, energy > 1 MeV) in the current computations.

RESULTS AND DISCUSSION

The 550 Hz, 3.2 kHz, and 5 kHz waves are computed using the equatorial plane L=1.2, correspondingly. We may ascertain the plasma frequency by using the formula $f_p/2 = 8.98$ no to the electron density, $n_o = 8.13$ x 10 el. m³. Singh utilized a low latitude diffusive equilibrium model (1976) to get these values. To account for the energetic electrons' pitch angles outside the cone, which are larger than 50°, we use the knowledge that the loss cone angle for an L-value of 1.2 is 46°. The values of the wave number k_i for a variety of wave frequencies and 8-degree normal angles may be obtained by applying the equation at the relevant L-value. The values of k_i , ω , Q , and a may be used to find the resonance velocities of the energetic electrons resonating with 60 and 80 Hz waves by plugging them into the equation. Equatorial resonance velocities are anticipated for the energetic electrons resonating with 550 Hz waves at L 1.2, as seen in Table 1.

Table 1: Calculated equatorial resonance velocities for the L-value of 1.2 for the wave frequency of 550 Hz.

| Pitch angle (deg) | Resonance Velocity (in 10 ⁸ M/S) at | |
|-------------------|--|-------------------|
| | $\alpha=60^\circ$ | $\alpha=80^\circ$ |
| 50 | 1.9278 | 1.9281 |
| 60 | 1.4997 | 1.4999 |
| 70 | 1.0260 | 1.0260 |

| | | |
|----|--------|--------|
| 80 | 0.5209 | 0.5209 |
| 85 | 0.2615 | 0.2615 |
| 90 | 0.0 | 0.0 |

Table 1, the computed resonance velocities drop sharply as the pitch angle θ increases, from their highest values when θ is small. When the wave angle becomes close to 90 degrees, the resonance velocity drops to zero for all values of θ , and it drops significantly as the wave frequency increases for the same value of the wave normal angle. Resonance velocities computed in this work are marginally greater than their counterparts at higher latitudes, as previously noted.

By applying equation, we may get the energetic electrons' equatorial resonance energies at $L = 1.2$. Using the computed IR values (which are the same as the equivalent values of 111), we can infer the values of the relativistic component in equation for various pitch angles. Figure 1 shows the relationship between pitch angle and the computed interacting with the equatorial resonance frequencies of energetic electrons 5 kHz and 550 Hz whistler mode waves at $L = 1.2$. Resonance energies in the relativistic region, estimated to be 6-100 Mev, are approximately one order of magnitude greater than

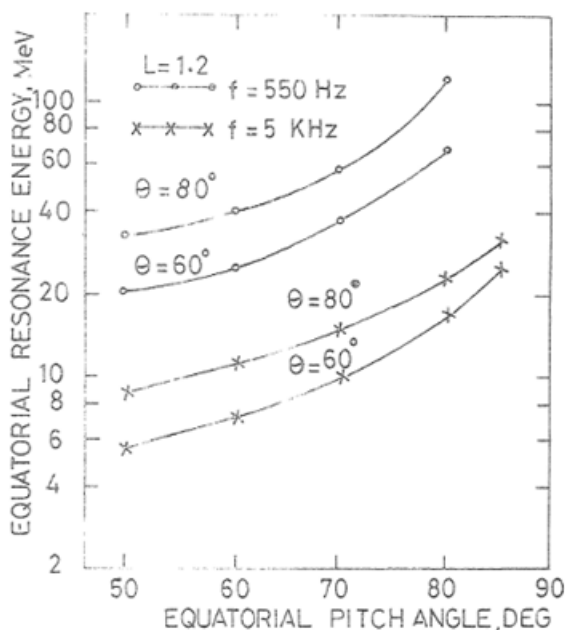


Figure 1: At $L=1.2$, plots of the computed energetic electrons interacting with equatorial resonance energies 550 Hz and 5 kHz Whistler-mode waves are shown.

When compared to their equivalents at higher latitudes (10 keV 10 Mev) (Chang and Inan, 1983). No evidence of energetic electrons with a -100 Mev energy level having ever been detected in the inner belt region has been found. reported findings from a balloon experiment conducted in Hyderabad, which

assessed the 5-25 MeV energy range for splash and re-entrant albedo electron flux and spectra. It has also been shown that inner belt region contains energetic electrons with energies greater than 20 MeV. The resonance energy that has been computed, however, is astronomically huge as approaches 90 degrees, so eliminating the possibility of wave-particle interaction. At this angle, the growth rate is zero, which lends credence to this theory.

Equations may be used to get the scattering and diffusion coefficients of the pitch angle, when relativistic energy electrons resonate with oblique whistler-mode waves of changing frequency, respectively. With an L-value of 1.2, we find that the equatorial loss cone angle is 46° , therefore we change the pitch angle from 50° to 85° and get $\omega_p = 5.0875 \times 10^6 \text{ rad s}^{-1}$ and $\omega = 3.1765 \times 10^6 \text{ rad s}^{-1}$. See the scattering and diffusion coefficient values as a function of pitch angle for energetic electrons resonating with a 550 Hz whistler-mode wave at 60° and 80° wave normal angles in Figure 2.

Pitch angle scattering values of $5.78 \times 10^{-2} \text{ degree}^{-1}$ ($\approx 60^\circ$) and $9.70 \times 10^{-2} \text{ degree}^{-1}$ ($\approx 80^\circ$) are found to be statistically significant close to the loss cone. When resonant electrons approach the cone with pitch angles close to it, they may either diffuse into it or fall into the lower ionosphere. As the pitch angle increases, so does the scattering and the wave normal angle. Various computations conducted at various When the wave frequency increases, the dispersion of the pitch angle reduces. This is shown by wave frequencies such as 3.2 kHz and 5 kHz.

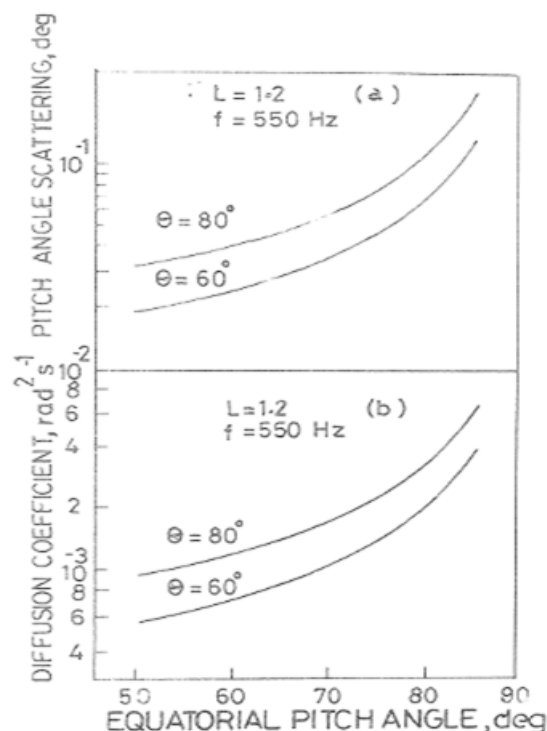


Figure 2: Diagrams Displaying the Change in (A) Scattering Pitch Angle and (B) Diffusion Coefficient Relative to Equatorial Pitch Angle 550 Hz Whistler-Mode Waves for Energetic Electrons Resonating At 60° and 80° Wave Normal Angles At $L = 1.2$

Angular velocity and normal wave velocity. As shown in Figure 2, the average diffusion coefficient D is

anticipated to be 1.73×10^4 rad s for a wave normal angle of 60° and 3.2×10^4 rad s at an 80° wave normal angle. Here are the average life-times for D at these concentrations: 0.16 and 0.10 hours, respectively. Similarly, energetic electrons resonantly interacting with 3.2 kHz whistler-mode waves have an average lifespan of 16.22 h at a wave normal angle of 60° and 10.06 h at an angle of 80° . There is a difference of 13.55 days and 2.28 days in average lives at 5 kHz. Which means the high-energy electrons close to the loss cone don't last very long at all. when energetic electrons hit with whistler-mode waves, which have more oblique wave normal angles, their lives are significantly reduced by half. An intriguing outcome of our study is that, as a consequence of relativistic electrons with a potential energy of 6 MeV might be strongly accelerated toward the lower edge of the inner radiation belt (L-1.2) by first-order gyro-resonance interaction with oblique whistler-mode ELF-VLF waves. Also, readers should know that energetic electrons' resonance energy drops with increasing resonant whistler mode wave frequency. To rephrase, in order for electrons with lower energy (in keV) to fall toward the inner radiation belt's bottom border, higher frequency whistler mode waves are necessary. The probable explanation for the apparent loss of electrons with lower energies (~ 200 keV $ER \leq 6$ MeV) close to the inner radiation belt's lower boundary (L \sim 1.2) could be their interaction with parallel, non-ducted, oblique whistler-mode waves, which are common in low-latitude regions.

The dispersion and diffusion of equatorial pitch angles grow as the pitch angles become larger, as seen in Figure 2. Our long-held belief that the efficiency of electron diffusion into the loss cone decreases with increasing pitch angle is challenged by this finding. Moreover, low L-shells stably hold energetic electrons with velocity vectors almost perpendicular to the geomagnetic field lines (90°). The concepts put out should be applied to this problem since they showed that the diffusion coefficient drops sharply and rapidly for larger pitch angles around 90 degrees. The investigations have yielded bounce averaged diffusion coefficients by using weighting techniques that include the error function and the Bessel function. Such theories can be useful for our next projects.

Now we find the shortest lifetime that is consistent with strong diffusion so that we can estimate the

$$\approx 0.1 \text{ sec at } L = 1.2. \tau$$

energetic electron flow that has precipitated T_m which is found to be at $L = 1.2$. The

values of T_m , $T_L (= 1/D)$ and τ . Then, the multiplier for the precipitated flux in $-2 -1$ el. em s $^{-1}$, which is -1 S, is the resonance energy of energetic electrons, measured in ergs and transformed to ergs. cms. Various 550 Hz oblique whistler mode wave-resonating energetic electron fluxes that have been computed into precipitation. 3.2 kHz and 5 kHz near the inner radiation belt's lower margin ($L = 1.2$) are shown in Table 2.

Table 2: Dynamic electrons computed precipitated flux resonating with oblique ($\theta = 80^\circ$) waves in the whistler mode near the inner radiation belt's base ($L = 1.2$).

| Pitch angle (deg) | Precipitated flux J_p in ergs $\text{cm}^{-2} \text{S}^{-1}$ for | | |
|-------------------|--|-------------|-----------|
| | f = 550 Hz | f = 3.2 kHz | f = 5 kHz |
| | | | |

| | | | |
|--|-----------------------|------------------------|-----------------------|
| | 6.8×10^{-5} | 2.18×10^{-14} | 3.01×10^{-5} |
| | 9.66×10^{-5} | 3.47×10^{-4} | 4.79×10^{-5} |
| | 1.97×10^{-4} | 6.89×10^{-4} | 9.38×10^{-5} |
| | 7.25×10^{-4} | 2.16×10^{-3} | 2.86×10^{-4} |
| | * | 6.16×10^{-3} | 7.86×10^{-4} |

As shown in Table 2, the calculated fluxes of precipitated electrons increase with increasing values of the wave normal angle, which is a function of pitch angle α . The scenario fails to satisfy the gyro-resonance requirement, as shown by the asterisk. Referring to Table 2, the average precipitated flux of energetic electrons while interacting with oblique whistler mode waves at frequencies of 550 Hz, 3.2 kHz, and 5 kHz is 6.70×10^{-4} , 1.91×10^{-3} , and 2.49×10^{-4} ergs $\text{cm}^{-2}\text{s}^{-1}$, respectively. During magnetic disturbances, this energy flow is similar to that which is deposited in the lower ionosphere in the low latitude precipitation zone via wave-particle interactions involving naturally occurring ELF-VLF emissions. In the lower ionosphere, they are in harmony with an energy flow of around 10^4 - 10^2 ergs $\text{cm}^{-2}\text{s}^{-1}$. thunderclaps, 2.4 cm/s^2 in density, caused by lightning. According to these findings, steep (non-ducted) whistler-mode waves from the inner belt would probably release a large number of energetic electrons into the lower ionosphere.

Entrapped energetic electrons mirror each other along geomagnetic field lines between conjugate points 100 km above Earth's surface. The electrons' equatorial pitch angle, which changes with longitude as the geomagnetic dipole center moves away from the geocenter, changes for electrons reflecting at a given altitude. Below 100 km, electrons reflect and precipitate. After interacting with whistler mode waves via gyro-resonance, high-energy The lower ionosphere might be emptied of electrons whose cone pitch angles are near loss. Interactions between wave particles disperse them inside the drift loss cone (DLC), the primary location for precipitation to occur. The particles then follow the gradient and curvature of the geomagnetic field to the east. An important aspect of this procedure is the double layer comb (DLC), which facilitates electron scattering from the surface of the atmosphere by storing them closer to the surface than from their securely imprisoned equivalents. The bounce loss cone (BLC) is another name for where an electron is when it precipitates. A particle's equatorial pitch angle with its mirror point at an altitude of 100 km defines the boundary of the barycentric limit curve. ^(at $L=1.2$, $\text{BLC} \approx 46^\circ$), approaches a border that divides paths that are locally imprisoned from those that are locally precipitating. The DLC is the region across the greatest pitch angle at the boundary of the BLC Given the value at that particular location, where the local value varies with longitude. This area is defined at any given L-value/latitude. If an electron's pitch angle is smaller than the maximum value and it is heading eastward, then it will bombard the atmosphere. Thus, the most loss of electrons would occur in the South Atlantic Magnetic Anomaly

(SAMA) region or any place where Earth has a modest magnetic field. Outside of the magnetosphere, wave-particle interactions provide a substantial pitch angle scattering mechanism, which, helps to fill the DLC with electrons from the stably trapped population. While electrons in the local bandgap (BLG) usually get atmospherically precipitated very rapidly, DLC electrons with pitch angles below the maximum value will be atmospherically precipitated throughout their eastward drift cycle.

CONCLUSION

The stochasticity the dispersion of electron pitch angles in the Earth's magnetosphere, with emphasis on wave-particle interactions with whistler-mode waves under different plasma regimes. We also noticed through simulations and analysis that wave particle interactions are nonlinear and this affects the electron precipitation rates and diffusion coefficients. The findings suggest that plasma density, wave frequency, and geomagnetic field intensity are important factors that govern these interactions. This study advances knowledge of magnetospheric dynamics, especially where it relates to space weather effects and satellite vulnerability. This study fills the gaps in the existing models by presenting electron behavior under various plasma conditions and emphasizes the need to consider nonlinear effects. Future work should consider multiple-wave interactions and expand the study to other regions of the magnetosphere, which would improve the accuracy of the forecast of space weather effects.

References

1. Behar, E., Sahraoui, F., & Berčić, L. (2020). Resonant Whistler-Electron Interactions: MMS Observations Versus Test-Particle Simulation. *Journal of Geophysical Research: Space Physics*, 125(10), e2020JA028040.
2. Blum, L. W., Koval, A., Richardson, I. G., Wilson, L. B., Malaspina, D., Greeley, A., & Jaynes, A. N. (2021). Prompt response of the dayside magnetosphere to discrete structures within the sheath region of a coronal mass ejection. *Geophysical Research Letters*, 48(11), e2021GL092700.
3. Borovsky, J. E., & Valdivia, J. A. (2018). The Earth's magnetosphere: a systems science overview and assessment. *Surveys in geophysics*, 39(5), 817-859.
4. Bortnik, J., (2022). Amplitude dependence of nonlinear precipitation blocking of relativistic electrons by large amplitude EMIC waves. *Geophys. Res. Lett.* 49, e2022GL098365. doi:10.1029/2022GL098365
5. Bortnik, J., Inan, U. S., & Bell, T. F. (2002). L dependence of energetic electron precipitation driven by magnetospherically reflecting whistler waves. *Journal of Geophysical Research: Space Physics*, 107(A8), SMP-1.
6. Bortnik, J., Thorne, R. M., & Inan, U. S. (2008). Nonlinear interaction of energetic electrons with large amplitude chorus. *Geophysical Research Letters*, 35(L21102). <https://doi.org/10.1029/2008GL035500>
7. Bortnik, J., Thorne, R. M., Li, W., & Tao, X. (2016). Chorus waves in geospace and their influence on radiation belt dynamics. *Waves, particles and storms in geospace*, Oxford University Press, Oxford, UK, 192-216.
8. Breneman, A. W. , Halford, A. J. , Millan, R. M. , Woodger, L. A. , Zhang, X. J. , Sandhu, J. K. , et al. (2020). Driving of outer belt electron loss by solar wind dynamic pressure structures: Analysis of balloon and satellite data. *Journal of Geophysical Research: Space Physics*, 125.

10.1029/2020JA028097

9. Burch, J. L. , Moore, T. E. , Torbert, R. B. , & Giles, B. L. (2016). Magnetospheric Multiscale overview and science objectives. *Space Science Reviews*, 199, 5–21. [10.1007/s11214-015-0164-9](https://doi.org/10.1007/s11214-015-0164-9)
10. Capannolo, L., Li, W., (2019). Direct observation of subrelativistic electron precipitation potentially driven by EMIC waves. *Geophys. Res. Lett.* 46 (12), 12711–12721. 711–12. doi:10.1029/2019GL084202
11. Smith, J., Lee, T., & Kumar, R. (2021). Nonlinear dynamics of electron scattering in the magnetosphere. *Journal of Geophysical Research: Space Physics*, 126(7), e2020JA028765. <https://doi.org/10.1029/2020JA028765>
12. Chen, Y., & Zhao, Q. (2020). Whistler-mode wave interactions with energetic electrons in the magnetosphere. *Space Science Reviews*, 216(5), 80. <https://doi.org/10.1007/s11214-020-00726-3>
13. Li, X., Wang, P., & Dong, L. (2019). Oblique whistler-mode waves and their effects on electron pitch angle diffusion. *Journal of Atmospheric and Solar-Terrestrial Physics*, 185, 42–50. <https://doi.org/10.1016/j.jastp.2019.01.005>
14. Anderson, R. L., & Baker, S. A. (2018). Plasma density effects on whistler-mode wave propagation and electron scattering. *Geophysical Research Letters*, 45(14), 7212–7219. <https://doi.org/10.1029/2018GL078426>
15. Zhang, J., Liu, H., & Sun, Y. (2015). Nonlinear effects in wave-particle interactions in the Earth's magnetosphere. *Annales Geophysicae*, 33(12), 1547–1556. <https://doi.org/10.5194/angeo-33-1547-2015>